OXFORD

Human Molecular Genetics, 2016, Vol. 25, No. 12 2578–2587

doi: 10.1093/hmg/ddw120
Advance Access Publication Date: 19 April 2016
Original Article

ORIGINAL ARTICLE

LSD1/KDM1A mutations associated to a newly described form of intellectual disability impair demethylase activity and binding to transcription factors

Simona Pilotto[1,†], Valentina Speranzini[1,†], Chiara Marabelli[1], Francesco Rusconi[2], Emanuela Toffolo[2], Barbara Grillo[2], Elena Battaglioli[2,3,*] and Andrea Mattevi[1,*]

[1]Department of Biology and Biotechnology, University of Pavia, 27100 Pavia, Italy, [2]Department of Medical Biotechnology and Translational Medicine, University of Milan, 20133 Milano, Italy and [3]CNR, Institute of Neuroscience, 20129 Milano, Italy

*To whom correspondence should be addressed at: Department of Medical Biotechnology and Translational Medicine, University of Milan, via Viotti 5, 20133 Milano, Italy. Tel: +390250315844; Fax: +390250335864; Email: elena.battaglioli@unimi.it (E.B); Department of Biology and Biotechnology "Lazzaro Spallanzani", University of Pavia, via Ferrata 1, 27100 Pavia, Italy. Tel: +390382985525; Fax: +390382528496; Email: andrea.mattevi@unipv.it (A.M.)

Abstract

Genetic diseases often lead to rare and severe syndromes and the identification of the genetic and protein alterations responsible for the pathogenesis is essential to understand both the physiological and pathological role of the gene product. Recently, *de novo* variants have been mapped on the gene encoding for the lysine-specific histone demethylase 1 (LSD1)/lysine(K)-specific histone demethylase 1A in three patients characterized by a new genetic disorder. We have analyzed the effects of these pathological mutations on the structure, stability and activity of LSD1 using both *in vitro* and cellular approaches. The three mutations (Glu403Lys, Asp580Gly and Tyr785His) affect active-site residues and lead to a partial impairment of catalytic activity. They also differentially perturb the ability of LSD1 to engage transcription factors that orchestrate key developmental programs. Moreover, cellular data indicate a decrease in the protein cellular half-life. Taken together, these results demonstrate the relevance of LSD1 in gene regulation and how even moderate alterations in its stability, catalytic activity and binding properties can strongly affect organism development. This depicts a perturbed interplay of catalytic and non-catalytic processes at the origin of the pathology.

Introduction

Histone lysine methylation is one of the most studied and characterized modifications, because it dynamically regulates multiple fundamental biological processes, including chromatin accessibility, transcription, DNA repair, cell cycle and development (1–4). Histone methylation is essential for the establishment of cell identity and maturation, as underlined by numerous studies on disease and tumorigenesis associated with mutations in either Lys methyltransferases or demethylases, as

[†]These authors equally contributed to this work.
Received: February 19, 2016. **Revised:** March 30, 2016. **Accepted:** April 8, 2016

well as in histone Lys residues (5). Likewise, novel sequencing studies are detecting mutations in different chromatin modifiers associated to neurodevelopmental disorders, showing how variations in chromatin regulation can be linked also to both intellectual and physical disabilities (6–8). In this context, functional alterations of lysine-specific histone demethylase 1 (LSD1/lysine(K)-specific histone demethylase 1A (KDM1A), hereafter referred to as LSD1), a H3-mono- (1) or di- (2) methylated lysine 4 demethylase, have been implied not only in a variety of physiological processes but also in pathological conditions, ranging from haematopoiesis impairment, neurological disorders and cancer (9–11). More recently, dominant missense point mutations in the *LSD1* gene (NM_001009999.2) have been identified, and correlated to a new genetic disorder that phenotypically resembles the Kabuki syndrome (OMIM 147920) but with distinctive facial features, skeletal anomalies and, above all, cognitive impairment (12,13).

In the reported case studies, three missense point mutations have been mapped on the *LSD1* gene: c.1207G > A predicting p.Glu403Lys (14), c.1739A > G encoding for Asp580Gly (14) and c.2353T > C, encoding for Tyr785His (13). The key issue is that these mutations represent *de novo* variants expected to be deleterious, as they affect residues in the catalytic core of the enzyme (Fig. 1). Indeed, the mutations are all in heterozygosis, indicating that they represent a dominant condition. This is especially interesting in light of the fact that the *LSD1* gene is essential, as demonstrated by mice homozygous mutants failing to develop properly after implantation (15,16).

With the aim of understanding how these newly identified pathological mutations affect the binding, catalytic, structural and repressive properties of this chromatin-associated enzyme, we produced and purified the three LSD1 disease-associated variants. Our combined analyses on the molecular features of the mutants both *in vitro* and *in vivo* provide new insights on how alterations of this epigenetic enzyme can translate into pathological conditions.

Results

LSD1 mutants are structurally stable yet catalytically impaired

For consistency with previously published works and to facilitate structural comparisons, the residue numbering used in the genetic studies for LSD1 protein (12–14) has been adapted to reference UniProt sequence O60341, which has been used so-far for all three-dimensional structures present in the Protein Data Bank. Therefore, the mutations Glu403Lys, Asp580Gly, Tyr785His will be hereafter referred to as Glu379Lys (E379K), Asp556Gly (D556G) and Tyr761His (Y761H). Domain and structural overview of recombinant LSD1-CoREST (corepressor of re1-silencing transcription factor) shows that these clinically relevant mutations all affect the active site. Glu379 and Asp556 are located towards the entry of the histone-tail binding site whereas Tyr761 occupies a more buried position to form the so-called aromatic cage, which is proximal to the flavin cofactor in the core of the catalytic centre (Fig. 1A).

We have recombinantly expressed, purified and characterized the three *de novo* LSD1 variants associated to pathogenic conditions. For all proteins, we performed co-purification with the corepressor CoREST, and in all cases this resulted in the same total recombinant protein yield in the range 1–3 mg/l of *Escherichia coli* culture, similar to LSD1 wild-type. All proteins showed no sign of folding instability (neither aggregation nor precipitation, as judged by gel filtration), therefore exhibiting the same tight association to CoREST. Similarly, thermal stability assays on the LSD1-CoREST complexes showed no significant changes in the unfolding melting temperatures (Table 1). Taken together, these results indicated that the pathological mutations do not affect the stability of the enzyme and its capability to bind to the co-repressor partner.

We next assessed the catalytic properties of the pathological LSD1 mutants. To test their ability to demethylate monomethylated-Lys4 of H3, we used a methylated peptide in a coupled assay (17). We found that D556G and Y761H are 10/20-fold less efficient compared with wild-type (essentially because of a decrease in the K_{cat}), whereas the activity of E379K is barely detectable, as listed in Table 2. To better understand if the decreased catalytic activities could be ascribed to a reduced binding affinity for histone H3 tail, we set up fluorescence polarization binding assays (Fig. 2). Furthermore, we assessed the thermal stability of LSD1 wild-type, E379K, D556G and Y761H LSD1 proteins in complex with CoREST when incubated with the same histone-derived peptide used for the enzymatic assays (Table 1). Both experimental approaches consistently indicated that LSD1 mutation E379K strongly impairs binding to the H3 N-terminal peptide, whereas mutations D556G and Y761H

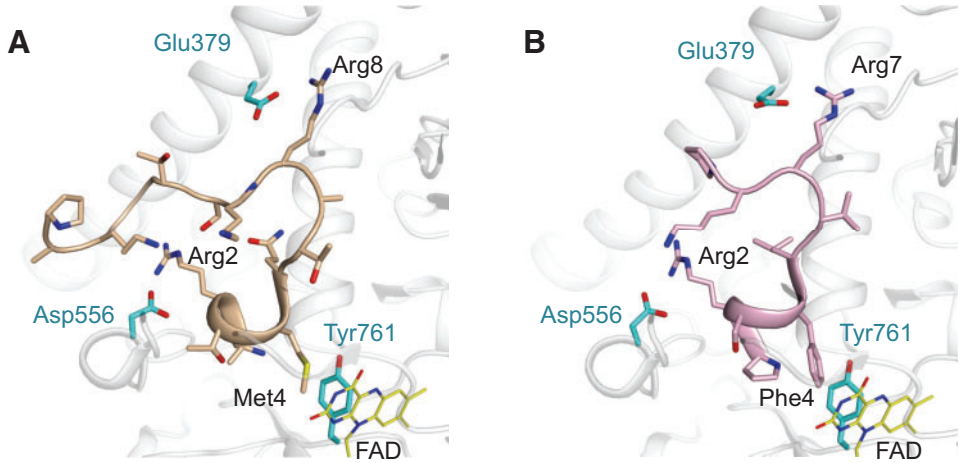

Figure 1. Structural analysis of Kabuki-like LSD1 mutations. Distributions in LSD1 (white) of the three residues affected by pathological mutations (cyan) and interactions with H3 tail substrate and interactor peptides. (**A**) Histone H3, depicted in wheat. The structure (PDB 2V1D) presents the histone peptide where Lys4 is substituted by a Met, mimicking demethylated product. (**B**) SNAIL1 (PDB 2Y48) in pink. Both substrate and the transcription factor peptides interact tightly with Glu379, Asp556 and Tyr761.

show binding similar to wild-type enzyme (Table 3). These biochemical assays were complemented by the elucidation of the three-dimensional structures of the LSD1 mutants in complex with CoREST (Table 4). The structures showed nearly identical quaternary arrangements, without overall or local conformational changes compared to the wild-type LSD1-CoREST native structure (Fig. 3). The conformation of both the catalytic and the FAD-binding sites is virtually identical in all structures, confirming the predicted positions of the pathogenic mutations in proximity to the H3 substrate binding site. Likewise, CoREST binding is indistinguishable from that observed in the wild-type enzyme, as expected from the biochemical analysis. Collectively, these investigations demonstrated that the mutations primarily affect enzyme catalysis and, to a minor extent, binding to the H3 N-terminal peptide without altering the protein conformation.

However, for the purpose of our analysis, it should be pointed out that each of the three alterations likely exerts its effect in a mutant-specific way. The strongest perturbation affecting substrate binding and catalysis is caused by E379K. Glu379 is directly involved in the recognition of Arg8 of histone H3 (Fig. 1A). It is conceivable that charge reversal at this locus essentially disrupts binding to the H3 N-terminal tail, which results in the mutant being enzymatically inactive. More subtle seem to be the effects of the other two mutations. Y761H affects a residue that is generally conserved among amine oxidases. Previous studies on human monoamine oxidases A and B have shown that a Tyr at this position creates a sterically and electrostatically favourable environment for the substrate amine group, promoting its oxidation (18). Indeed, the Tyr-to-His mutation in monoamine oxidases decreases the catalytic efficiency and the same effect is now found in LSD1 (Tables 2). D556G is the mutation with the milder consequences on the enzyme biochemical properties as it features only a 10-fold reduced K_{cat}. Asp556 is part of a cluster of negatively charged residues that interact with Arg2 of the H3 N-terminal tail (Fig. 1A). The D556G mutations still allows the active site to engage histone tail (Table 3). Likely, removal of the negatively charged Asp side chain leads to a non-productive histone binding conformation, which does not allow the correct positioning of methylated Lys4 to face the flavin for efficient oxidative demethylation.

These data are supported by experiments performed with nucleosomal particles bearing a propargyl methyl-Lys4 analogue. These semisynthetic nucleosomes effectively function as a suicide substrate whose modified H3-Lys4 forms a covalent adduct with the flavin cofactor upon binding to the enzyme (19). Consistently with the non-productive binding of the H3 tail, all three pathogenic mutations hamper the covalent reaction between the modified Lys4 and the LSD1 flavin cofactor, as none

Table 1. Thermal stability assays with LSD1-CoREST wild-type and mutants[a]

	No ligand[b]	H3 (1–21)	SNAIL1 (1–9)
LSD1-CoREST	0 (T_m=50.5)	+ 2.5	+ 7.5
$LSD1_{E379K}$-CoREST	+1.5	+0.5	+4.5
$LSD1_{D556G}$-CoREST	+1	+1.5	+10.5
$LSD1_{Y761H}$-CoREST	+2	+1.5	+2.5

[a]All temperature shifts are reported in °C and refer to the T_m value measured in the absence of ligands. H3 (1–21) is the Lys4-methylated H3 peptide corresponding to residues 1–21 of H3. SNAIL1 (1–9) is a peptide with sequence corresponding to residues 1–9 of human SNAIL1.

[b]The melting temperature (T_m) of the wild-type protein is in brackets. Temperature shifts refer to the T_m value measured for the wild-type in the absence of ligands.

Table 2. Kinetic parameters for activity of LSD1-CoREST wild-type and mutants[a]

	K_m (μM)	K_{cat} (min^{-1})	K_{cat}/K_m (min^{-1}/μM)
LSD1-CoREST1	3.89 ± 0.43	4.72 ± 0.16	1.21 ± 0.15
$LSD1_{E379K}$-CoREST	n.d.[b]	<0.01	n.d.[b]
$LSD1_{D556G}$-CoREST	2.55 ± 0.45	0.30 ± 0.01	0.12 ± 0.21
$LSD1_{Y761H}$-CoREST	1.28 ± 0.26	0.18 ± 0.01	0.14 ± 0.25

[a]All experiments were performed in quadruplicate.

[b]n.d., not detectable because of too low activity.

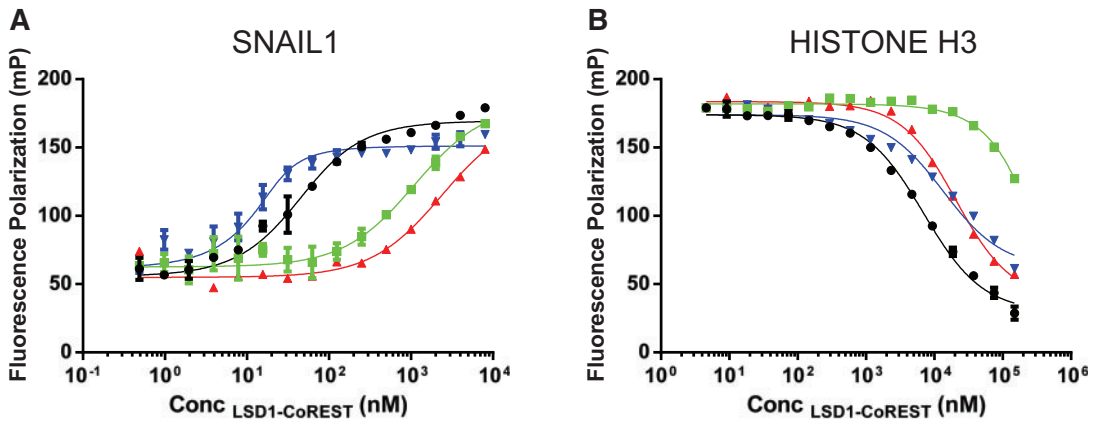

Figure 2. LSD1-CoREST mutants bind differently to histone substrate and transcription factor SNAIL1. Binding properties of LSD1 wild-type (black), Glu379Lys (green), Asp556Gly (blue) and Tyr761His (red; in complex with CoREST) to histone H3- and SNAIL-derived peptides. (**A**) Increasing concentrations of purified LSD1-CoREST wild-type and mutants were incubated with 5(6)-carboxytetramethylrhodamine-conjugated SNAIL1 N-terminal peptide (residues 1–9). Changes in polarization were measured in millipolarization (mP) units and plotted against the concentration of LSD1-CoREST. The corresponding K_d values are reported in Table 3. (**B**) Binding to me_2Lys4 1-21 H3 N-terminal peptide was measured in competition against SNAIL1. LSD1-CoREST wild-type and mutants were incubated with increasing (0–150 μM) concentrations of competing H3 peptide. Comparison with the curve and K_d values obtained by direct binding (A, black) allowed affinity measurements and K_d calculation, as reported in Table 3. Both in A and in B, error bars correspond to standard deviations for all measurements ($n \geq 3$). The choice of using SNAIL1 (instead of H3) for direct binding is based on the proven higher affinity for this peptide (19,28), which allowed a larger dynamic range of affinity.

Table 3. Affinity of LSD1-CoREST wild-type and mutants to histone and SNAIL1 peptides[a]

	H3 (1–21) K_d (μM)	SNAIL1 (1–9) K_d (μM)
LSD1-CoREST	3 ± 0.3	$3.43 \cdot 10^{-2} \pm 5.8 \cdot 10^{-3}$
$LSD1_{E379K}$-CoREST	> 150	1.1 ± 0.3
$LSD1_{D556G}$-CoREST	3.8 ± 1.3	$4 \cdot 10^{-3} \pm 1.8 \cdot 10^{-3}$
$LSD1_{Y761H}$-CoREST	9.8 ± 4.1	2.4 ± 0.9

[a]All experiments were performed in quadruplicate.

Table 4. Crystallographic data collection and refinement statistics for LSD1-CoREST mutants

	E379K	D556G	Y761H
PDB code	5L3C	5L3B	5L3D
Unit cell (Å)[a]	120.4, 180.4, 235.4	119.1, 179.1, 234.4	120.3, 177.7, 235.2
Resolution (Å)	3.3	3.3	2.6
R_{sym} (%)[a,b]	13.0 (81.0)	13.1 (61.3)	7.6 (97.0)
$CC_{1/2}$[b,c]	0.99 (0.47)	0.99 (0.71)	1.00 (0.52)
Completeness (%)	99.0 (99.0)	99.6 (99.9)	99.2 (100.0)
Unique reflections[b]	38276 (4604)	37869 (4593)	76680 (4596)
Redundancy[b]	3.8 (3.9)	3.8 (3.8)	4.4 (4.5)
Average Intensity/σI[b]	8.5 (1.2)	7.2 (1.7)	10.5 (1.0)
Number of protein atoms	6356	6342	6344
Number of solvent atoms	0	0	64
Ramachandran favoured (%)	96.3	96.0	96.9
Ramachandran allowed (%)	3.5	3.4	2.9
Ramachandran outliers (%)	0.2	0.6	0.2
Rwork (%)[d]	19.9	19.5	20.8
Rfree (%)[d]	22.3	20.8	21.9
Rmsd bond length (Å)	0.009	0.020	0.009
Rmsd bond angle (°)	1.40	1.30	1.20

[a]For all structures, space group is I222. $R_{sym}=\sum|I_i-\langle I\rangle|/\sum I_i$, where I_i is the intensity of ith observation and $\langle I\rangle$ is the mean intensity of the reflection.

[b]Values in parentheses are for reflections in the highest resolution shell.

[c]The observed resolution limits of the diffraction data were selected by evaluating the mean(I) correlation between half datasets, as defined by Karplus and Diederichs (44).

[d]$R_{work}=\sum||F_{obs}|-|F_{calc}||/\sum|F_{obs}|$ where F_{obs} and F_{calc} are the observed and calculated structure factor amplitudes, respectively. R_{work} and R_{free} were calculated using the working and test sets, respectively.

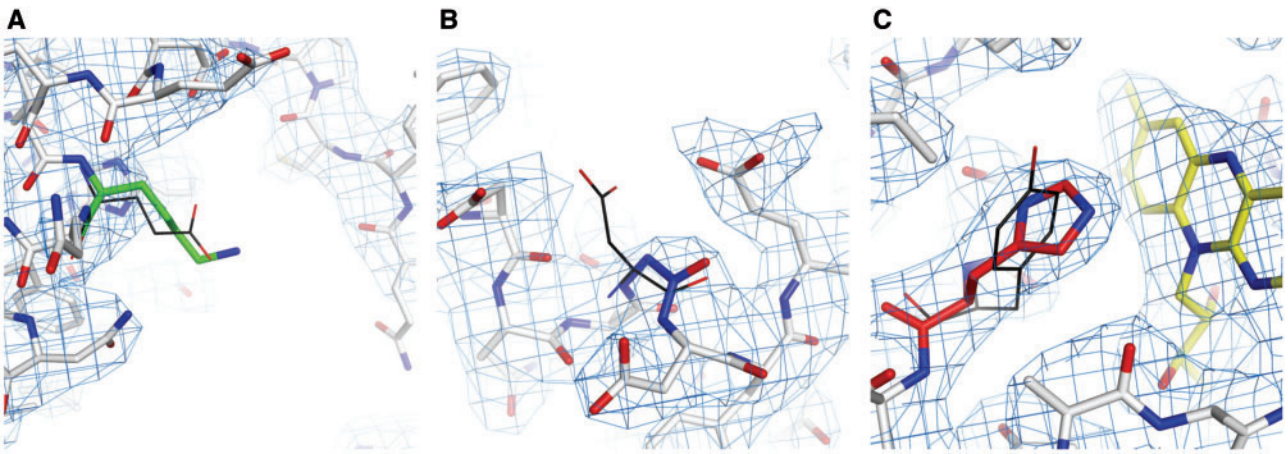

Figure 3. Three-dimensional structure of LSD1 pathological mutants. Distributions in LSD1 of each of the three residues affected by pathological mutations. Structures are compared to wild-type (black, thin line). (**A**) Glu at position 379 is substituted with a Lys (green), whose side chain shows to be disordered due to the lack of defined electron density. (**B**) Asp at position 556 is mutated to a Gly (blue). (**C**) Tyr at position 761 is replaced by a His (red). Electron density 2Fo-Fc map of each mutant LSD1 is represented as blue grid at contour level of 1.2σ.

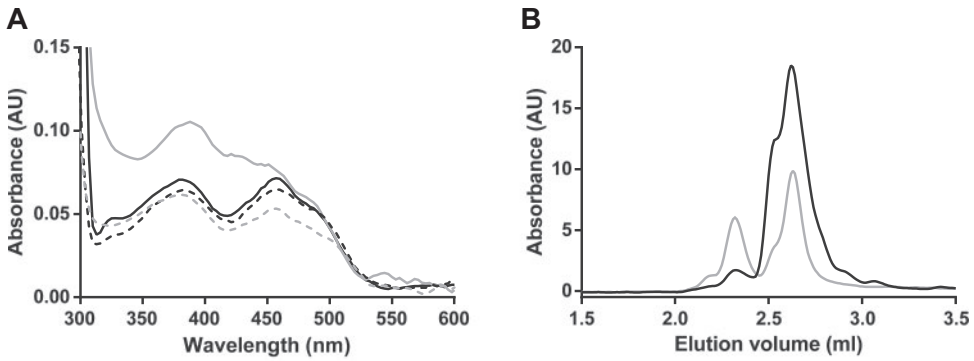

Figure 4. Pathological mutations in LSD1 hamper the binding to nucleosomal particles. (**A**) Wild-type (dashed grey) and mutant (dashed black, for simplicity only D556G mutant is shown) LSD1-CoREST (25 μM) show the typical absorbance peaks at 380 and 458 nm of the oxidized FAD. Binding of propargyl-modified H3 nucleosomes to wild-type LSD1 causes a spectral change with the formation of a single peak close to 400 nm (solid grey). Upon interaction with modified nucleosomes, the mutant spectra (solid black with reference to D556G) are unaltered, indicating no covalent binding to the FAD. (**B**) This observation was confirmed when purification of the covalent $LSD1_{D556G}$-CoREST-nucleosome was attempted. The analytical gel filtration chromatogram shows that LSD1 wild-type (grey) forms a 1:1 covalent complex with the nucleosome (elution volume 2.3 ml), whereas mutants (black, for simplicity only D556G mutant is shown) only show the elution profiles of free nucleosomes (2.6 ml) and free LSD1-CoREST (2.7 ml).

of the mutants are able to form such a stable complex with the modified nucleosomes (Fig. 4).

LSD1 inactive mutants retain the ability to associate to corepressor partners and gene repression capability in cell lines

LSD1 transcriptional repressive capability is tightly linked to and dependent on its association with corepressors histone deacetylase 1/2 (HDAC1/2) and CoREST inside the nucleus (20–23). We initially confirmed nuclear localization of hemagglutinin (HA)-tagged LSD1 mutants in non-neuronal and neuronal cells (Fig. 5A). Next, we assessed the ability of LSD1 mutants to recruit a proper corepressor complex through HDAC1/2 and CoREST binding in human cells. We transfected each HA-tagged LSD1 mutant into Henrietta Lack (HeLa) cells and then probed HA-immunoprecipitates for LSD1 association with endogenous HDAC1, HDAC2 and CoREST. All three mutants showed deacetylase and corepressor binding comparable to wild-type HA-LSD1 (Fig. 5B), in agreement with the biochemical and structural studies.

We then functionally assessed the effect of the mutations in a cell-based transcriptional assay by generating Gal4-LSD1 mutants that were transfected together with 5xUAS–TK–LUC reporter gene in HeLa and neuroblastoma SH-SY5Y cell lines (Fig 5C–E). For each mutant, the repressive activity was measured as *Luciferase* expression normalized over a cotransfected *Renilla* reporter. The repressive behaviour was ascertained as residual luciferase activity compared to the empty Gal4-vector, which was arbitrarily set to 100%. In parallel with the pathological mutations, we used the same assay to analyse the effect on transcription of a previously characterized enzymatically inactive LSD1 mutant, K661A, specifically designed to interfere with demethylase reaction (21,24). As shown in Figure 5C, Gal4-LSD1 K661A displayed a modest although significant reduction in repressive activity in HeLa cells compared with Gal4-LSD1, while in the neuronal cell context the effect of the inactivating mutation was stronger. Repressive activities of Gal4-LSD1 and Gal4-LSD1 K661A defined the dynamic range in which to evaluate demethylase-dependent transcriptional modulation induced by the three pathological mutations. Gal4-LSD1 D556G, Y761H and E379K did not substantially differ when compared to wild-type Gal4-LSD1. Only Gal4-LSD1 E379K showed a slight, yet significant, impairment of the repressive activity in HeLa cells, similarly to LSD1 K661A (Fig. 5C). The ability of LSD1 mutants to retain repressive capacity could be ascribed to the unaltered hallmark of all LSD1 mutants to efficiently interact with HDAC1/2 and CoREST in corepressor complexes (Fig. 5B). Collectively, these data suggest that, at least in this system, substantial impairment of the LSD1 demethylase activity does not affect repression of the target reporter gene. Consistently, previously reported experiments on the LSD1 K661A mutant showed that also this catalytically inactive enzyme is able to retain full association with the breast cancer type 2 susceptibility protein (BRCA2)-associated factor-HDAC complex, responsible for the repressive activity towards target genes (25).

LSD1 mutations reduce protein stability in vivo

Having observed that, despite being catalytically impaired, the mutants retain substantial repressive activity, we next investigated whether LSD1 stability is affected by the pathological mutations in human cell lines. This question was addressed by probing protein levels in HeLa cells after blocking protein synthesis via cycloheximide administration to the culture media (26), followed by time-course comparisons with the wild-type protein (Fig. 6). In our experimental conditions, HA-LSD1 displays a half-life of ∼33 h. Interestingly, all mutants showed substantially shortened half-life, ranging from 15 h for Y761H down to 9 and 5.5 h for D556G and E379K, respectively. Such a significant reduction in protein levels will potentially add to the effects on catalytic and binding properties, contributing to the pathological phenotype associated to these mutations.

Pathological mutations in LSD1 have different effects on binding to transcription factors

To further examine the properties of LSD1 E379K, D556G and Y761H, we assessed their capability to bind the transcription factor zinc finger protein SNAI1 (SNAIL1), which is implicated in the differentiation of epithelial cells into mesenchymal cells during embryonic development (27). SNAIL1 and similar

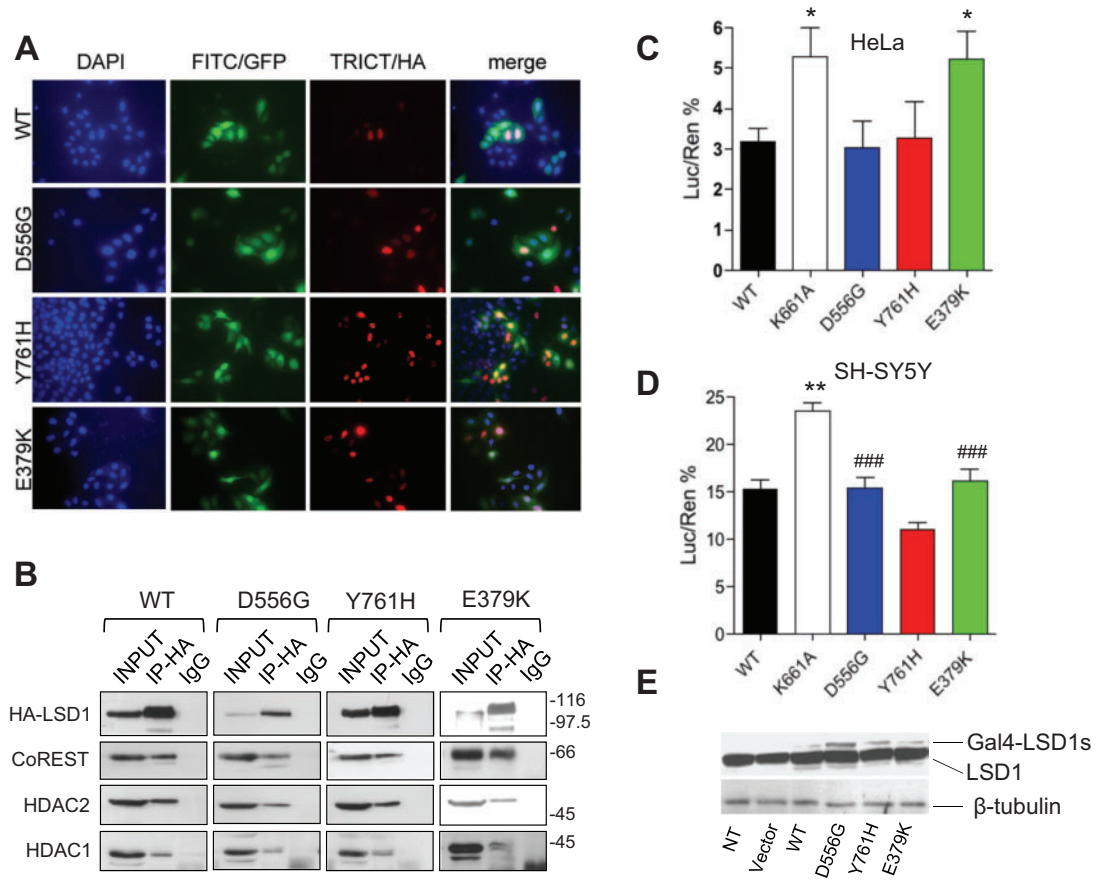

Figure 5. Effect of patient mutations on LSD1 repressive activity. (**A**) LSD1 D556G, Y761H and E379K do not alter LSD1 nuclear localization in HeLa cells. Immunofluorescence analysis of transiently expressed HA-LSD1 and annotated HA-tagged mutants co-transfected with EGFP, stained with anti-HA antibody. Nuclei are evidenced with DAPI staining (magnification 40×). (**B**) In human cell lines, LSD1 mutants retain the ability to bind to corepressors HDAC1/2 and CoREST. Protein extracts from HeLa cells transfected with HA-tagged LSD1 and related mutants (HA-LSD1-D556G, HA-LSD1-Y761H, HA-LSD1-E379K) immunoprecipitated with anti-HA antibody or pre-immune IgG, separated on SDS–PAGE and immunodecorated with HA, CoREST, HDAC1 and HDAC2 antibodies. (C-D) LSD1 and LSD1 mutants D556G, Y761H, E379K together with the demethylase-dead mutant LSD1 K661A, fused to Gal4, were assayed for their ability to repress the 5xUAS-TK-LUC reporter gene in (**C**) HeLa cells at 1:0,125 reporter:repressor molar ratio and in (**D**) neuroblastoma SH-SY5Y cells at 1:2 reporter:repressor molar ratio. The *Luciferase* activity normalized on the co-transfected *Renilla* reporter was expressed as a percentage of the Gal4 empty vector put to 100% (not shown). Mean values ± SE are shown. Student's *t* test was applied to percentage values (*refers to LSD1-WILD-TYPE; # refers to LSD1-K661A). $^{*}P < 0.05$; $^{**}P < 0.01$; $^{###}P < 0.001$. (**E**) Protein expression of LSD1 and mutant proteins, normalized on β-tubulin level.

transcription factors are known to recruit the repressive complex LSD1-CoREST-HDAC to their target gene promoters through binding to LSD1 active site, mimicking the histone H3 N-terminal tail (28,29). We performed thermal stability and binding assays using a peptide corresponding to the N-terminal tail of SNAIL1, whose sequence is strictly conserved in all members of SNAIL1-related family (30) (Tables 1 and 3). From these experiments, it emerged that the three pathological mutations differentially affect binding to SNAIL1: two of them (E379K and Y761H) drastically reduce affinity (> 30-fold; Table 3), whereas D556G features little variations compared to the wild-type enzyme.

These findings can be rationalized in light of the three-dimensional structure of LSD1-CoREST bound to SNAIL1 (Fig. 1B) (28). Removal of Asp556 negatively charged side chain (D556G) has no effect on transcription factor binding. A plausible explanation to this observation is that a glycine at this position may allow solvent molecules to interact with SNAIL1 Arg2 side chain, with little effect on the overall binding affinity for the transcription factor. A similar effect is observed on the affinity for the H3 peptide, although the precise histone binding mode and efficiency is likely affected, as shown by reduced K_{cat} rates. In contrast, E379K mutation profoundly affects SNAIL1 binding by reversing the charge of Glu379 which normally interacts with Arg7 of SNAIL1. Again, such a strong perturbation matches the drastic effect by this mutation on H3 binding. More specific is the impact on SNAIL1 binding induced by Y761H. In this case, a polar histidine side chain affects the characteristic hydrophobic interaction between the aromatic rings of Phe4 of SNAIL1 and Tyr761 of LSD1 (Fig. 1B). Hence, the Y761H mutation has a much stronger effect on SNAIL1 binding (70-fold decrease in affinity) compared with H3, which features a Lys (Lys4) rather than a Phe in direct contact with Tyr761. These data demonstrate how active-site mutations can differentially perturb binding of histone tail and histone-mimicking transcription factors.

Discussion

Exon sequencing data allowed the identification in three young patients of three different point mutations affecting residues in the active site of the histone demethylase LSD1 (12–14). In this work, we show that all of these mutations negatively influence both the demethylase catalytic efficiency and cellular protein stability, though to different extents. In contrast, these LSD1

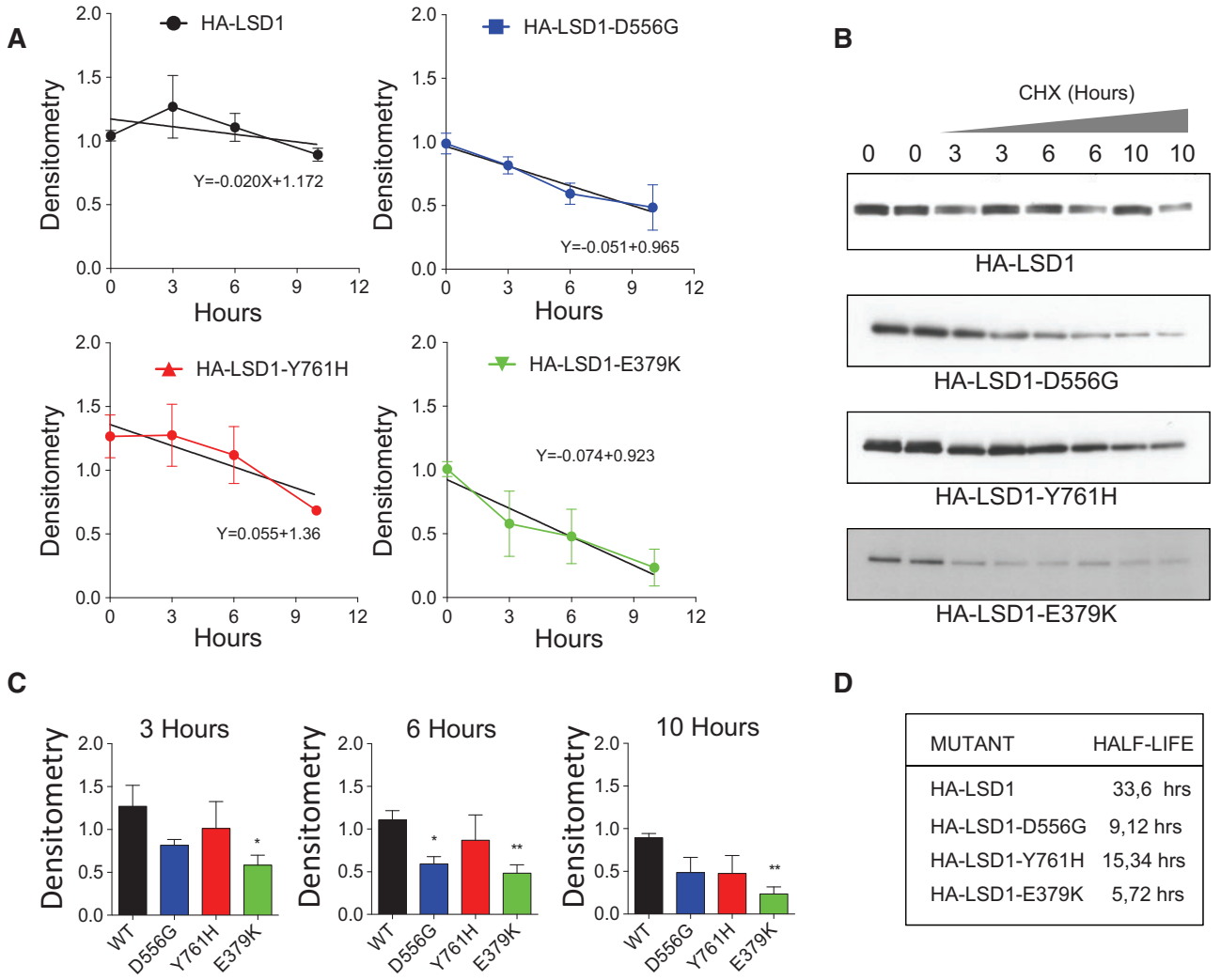

Figure 6. Pathological mutations destabilize LSD1 protein. Cycloheximide (CHX, 100 μg/ml) time-courses stability assay on HeLa cells transfected with HA-LSD1, HA-LSD1-D556G, HA-LSD1-Y761H or HA-LSD1-E379K show that mutant LSD1 isoforms are less stable than the wild type. (**A**) Linear regression analysis of time course densitometry experiments relative to wild-type LSD1 and mutants. (**B**) Representative western blot films for wild type LSD1 and mutant isoforms. A loading control for each transfected cell line was performed (not shown). (**C**) Time-courses densitometry analysis relative to the untreated cells of each transfected HA-LSD1 and mutated isoforms. (**D**) Inferred protein half-lives. Mean values ± SE are shown. Student's *t* test was applied. $^{*}P < 0.05$; $^{**}P < 0.01$ referred to WT HA-LSD1.

mutations retain repressive activity on a reporter gene, most likely due to unaltered binding to the co-repressors HDAC1/2 and CoREST. Therefore, as H3-Lys4 methylation is a widespread and key epigenetic mark, alteration in its homeostasis and reprogramming is seemingly the main reason for the extensive developmental effects observed in the patients affected by the newly discovered pathologic condition caused by LSD1 mutations (12). Thus, the enzymatic histone demethylase activity is far from being dispensable for proper development, as already reported in literature for either embryonic stem cells and haematopoietic differentiation or for the establishment of proper neuronal identity (22,31–34).

Notwithstanding its catalytic function, LSD1 can also recognize and bind a variety of non-histone ligands, ranging from other chromatin modifiers such as transcription factors and the tumour suppressor p53 (10,21,29,35). In this work, we found that the pathological mutations do affect such interactions, with a focus on the binding to SNAIL1, known as a master regulator of the epithelial–mesenchymal transition during development and tumour progression. Indeed, this binding is deeply affected by two (Y761H and E379K) of the analysed mutations, which can further contribute to the pathogenesis. In this context, it cannot be excluded that pathological effect of D556G is exacerbated by adverse alterations on the binding to interactor(s) other than SNAIL1-related factors. For instance, it has been recently shown that the neuro-specific splicing variant of LSD1 (22) might be endowed with the ability to demethylate other Lys residues such as H3-Lys9 or H4-Lys20, depending on the interaction with specific co-repressor or co-activators different from CoREST. We cannot exclude that also these regulatory interactions could be affected by the mutations, impairing neuro-specific roles of LSD1 (36,37). Hence, it is clear that the function of the active site of LSD1 is not limited to the recognition and modification of the methylated histone H3 tail. Rather, it is a hub for competitive interactions with the nucleosomal tails as well as transcription factors, implying that even catalytically and biochemically mild mutations targeting this protein region can have pleiotropic (both catalytic and non-catalytic) effects. Along this line, it has been very recently demonstrated that simply a partial loss of maternal LSD1 demethylase is

sufficient to block maternal oocytes epigenetic reprogramming, leading to deregulated gene expression during embryonic maturation and consequentially developmental aberrations at birth (38). In conclusion, LSD1 and associated factors are such key players in establishing and maintaining patterns of chromatin modifications that a moderate reduction in enzymatic activity and protein levels lead to severe pathological conditions.

Materials and Methods

Protein expression and purification

LSD1 mutants were prepared using standard mutagenesis procedures (QuickChange Mutagenesis Kit, Agilent Technologies Milano, Italy), and purified as the wild-type proteins. Protein expression and purification of all constructs were performed using previously published protocols (39).

Thermal stability assays

Protein thermostability was tested using ThermoFAD as previously described (40). All proteins were incubated at 4 μM final concentration together with peptides (H3 1–21 and SNAIL1 1–9; Table 1) at 200 μM final concentration in 50 mM 4-(2-hydroxyethyl)-1-piperazineethanesulfonic acid (HEPES)/NaOH pH 7.5 and stability was assessed over a temperature range 20–90°C.

LSD1 activity assays

Enzymatic activities were evaluated by a peroxidase-coupled assay monitoring hydrogen peroxide formation (39). The reaction mixture contained 50 mM HEPES/NaOH pH 7.5, 0.1 mM Amplex Red, 0.3 mM horseradish peroxidase, 0.1 μM LSD1-CoREST and varying concentrations of monomethylated H3 – K4 peptide substrate (0.3–40 μM). Fluorescence changes following the conversion of Amplex Red (Invitrogen ThermoFisher Scientific) to Resorufin were monitored at 535 and 590 nm for excitation and emission, respectively. Assays were performed at 25 °C in 96-plate format using a CLARIOstar plate reader (BMG Labtech, Germany). Initial velocity values were fitted to Michaelis–Menten equations.

Fluorescence polarization binding assays

Binding assays to LSD1-CoREST wild-type and mutants were carried out monitoring the change in polarization properties of SNAIL1 peptide (amino acids 1-9) fluorescently labelled with 5(6)-carboxytetramethylrhodamine (TAMRA) as previously described (19). Briefly, all experiments were carried out in 15 mM KH_2PO_4 pH 7.2, 1 mg/ml BSA, 5% glycerol at 25 °C. CLARIOstar (BMG Labtech, Germany) plate reader was used with 540 nm excitation and 590 nm emission filters. Experiments were performed in triplicates using 384-well microplates (CORNING, UK). Direct binding of SNAIL1-TAMRA at a final concentration of 10 nM was performed to calculate K_d values. LSD1-CoREST was kept constant at 30 nM for wild-type, 1 μM for E379K, 3 nM for D556G, 2.5 μM for Y761H. For competitive experiments, each well contained LSD1-CoREST at the listed concentrations and labelled peptide (10 nM final). Next, decreasing concentrations (typically in the 0–150 μM range) of the unlabelled competing H3 peptide (ARTme$_2$KQTARKSTGGKAPRKQLA) was added to the wells mixture and competitive curves recorded with the same settings.

Binding to semi-synthetic nucleosomes

Nucleosome binding by LSD1-CoREST wild-type, E379K, D556G and Y761H was performed by incubating each protein with semi-synthetic recombinant nucleosomes, which were prepared as previously described (19). LSD1-CoREST proteins (in 25 mM KH_2PO_4 pH 7.2, 5% glycerol) were mixed with semi-synthetic nucleosomes (in 20 mM Tris(hydroxymethyl)aminomethane (Tris)/HCl pH 7.5, 1 mM (ethylenedinitrilo)tetraacetic acid (EDTA), 1 mM 1,4-dithiothreitol (DTT)) at 1.5:1 molar ratio and incubated on ice for 1 h. Absorbance spectra were recorded in the UV-visible range of wavelengths using the NanoDrop spectrophotometer (ThermoScientific). Analytical size-exclusion chromatography was performed for each mix on silica gel column WTC-030N5 (4.6 × 300 mm) (Wyatt Technology, CA) equilibrated in buffer 200 mM KCl and 10 mM Tris/HCl pH 7.5 (4°C). Detection wavelength were set at 214 nm (peptide bond), 260 nm (DNA) and 280 nm (aromatic protein side chains) and elution profiles were recorded using an AKTAmicro purification system (GE Healthcare). Figure 4B shows only the 214 nm profiles for graphical simplicity.

X-ray crystallography and structural analysis

Crystals of mutant LSD1-CoREST complexes were obtained at 20 °C as previously described (39). X-ray diffraction data were collected at 100 K at beamline X06DA at the Swiss Light Source (SLS, Villigen, Switzerland) and at beamline ID23-1 at the European Synchrotron Radiation Facility (ESRF, Grenoble, France). Data processing and crystallographic refinement were carried out with standard procedures using XDS (41) and programs of the CCP4 suite (42). Atomic co-ordinates for the E379K, D556G and Y761H mutants have been deposited in the Protein Data Bank with accession codes 5L3B (D556G), 5L3C (E379K), 5L3D (Y761H) (Table 4). Structural figures were prepared using PyMOL (The PyMOL Molecular Graphics System, Schrödinger, LLC).

Cell cultures

HeLa and SH-SY5Y cells were, respectively, cultured in Dulbecco's modified Eagle's medium (DMEM) and Roswell Park Memorial Institute (RPMI) medium supplemented with 10% fetal bovine serum, 1% penicillin/streptomycin and 1% glutamax. Cycloheximide was solubilized in DMSO and used at 100 μg/ml to block HeLa cells protein synthesis. For stability assays, transfected cells were seeded 24 h upon transfection (day 1) in four different wells, one for each condition (control, 3–6 and 10 h treatment with cycloheximide). On day 2, cells were collected at different time points and analysed by western blot (26).

Plasmids and transfection

Gal4-LSD1 fusion constructs containing full-length LSD1 as well as pCGN vectors encoding HA-LSD1 have been described elsewhere (22,24). LSD1-K661A, D556G, Y761H and E379K were obtained by site-specific mutagenesis using as template Gal4-LSD1 and pCGN-HA-LSD1 plasmids with QuikChange II Site-Directed Mutagenesis Kits (Stratagene, La Jolla, CA, USA). All plasmids were sequenced. HeLa and SH-SY5Y cells were transiently transfected using Lipofectamine 2000 (Invitrogen, Waltham, MA, USA) and processed for transcription repression assay after 48 h. For stability and immunoprecipitation assays, transfection was performed with Lipofectamine LTX (Invitrogen) according to manufacturer's instructions.

Immunoprecipitation assays

Experiments were performed as reported (24). Briefly, HeLa cells protein extraction was performed in low-stringency buffer (10% glycerol, NaCl 150 mM, imidazole 10 mM, 0.5 mM EDTA 0.5% Triton-X100, DTT 0.5 mM) supplemented with 1 mM phenylmethanesulfonyl fluoride and 1× Protease Inhibitors Cocktail (Roche) and 1× Phosphatase Inhibitor Cocktail (Roche). 0.5 mg of cell extract were used and collected with HA-conjugated Agarose beads (Santa Cruz, Santa Cruz, CA). After incubation, beads were washed with IP buffer, immunoprecipitates eluted with 1X sodium dodecyl sulphate (SDS) Sample buffer and processed for western blot. Quantification was performed using ImageJ software. Western blotting experiments were performed as previously described (43). Lysates and immunoprecipitates were resolved on 8% SDS–PAGE (polyacrylamide gel electrophoresis) gels whereas for LSD1 stability assays, HA-LSD1 and HA-LSD1 mutants were resolved on 7% SDS–PAGE gels. Antibodies were the following: Anti LSD1 (C69G12 CST, Denver, MA, USA); anti CoREST (07-455 Merck Millipore, Billerica, MA, USA); anti-HDAC2 (ab7029 Abcam, Cambridge, UK); anti-HDAC1 (ab7028 Abcam, Cambridge, UK) anti-α/β Tubulin (2148 CST, Danvers, MA, USA), anti-HA (sc-7392 and sc-80 Santa Cruz Biotechnology, CA, USA).

Repression assays

5xUAS-TK-LUC reporter plasmid (24) was used at the indicated molar ratio relative to the expression plasmids pGal4-LSD1 and pGal4-LSD1 mutants. Control experiments were carried out by using equivalent molar amounts of pGal4 empty vectors. DNA was maintained constant through pBSIIKS buffering (Stratagene, La Jolla, CA, USA). pRL-TK-reporter vector (Promega, Madison, MI, USA) was used to normalize for transfection efficiency. The luciferase reporter activity was determined with the Dual-Luciferase reporter assay system (Promega) according to the manufacturer's instructions. Values of *Firefly* luciferase were normalized over *Renilla* luciferase (both expressed as relative luminescent units). The activity of each construct was expressed as a percentage of the pGal4 empty vector.

Nuclear localization in cells

HeLa cells were transfected using Lipofectamine 2000 (Invitrogen). After 2 days cells were fixed with a PBS solution containing 4% paraformaldehyde for 10 min. Cells were incubated with anti-HA (sc-80) for 3 h in GDB buffer (30 mM phosphate buffer, pH 7.4, containing 0.2% gelatin, 0.5% Triton X-100 and 0.8 M NaCl), followed by 1 h incubation with cyanine 3-conjugated secondary antibody (The Jackson Laboratory, USA) and mounted in VectaDAPI medium (Vector Laboratories, USA). Images were acquired using Nikon Eclipse E600 microscope.

Acknowledgements

We acknowledge SLS and ESRF for provision of synchrotron radiation facilities and their staff during data collection. We thank Dr. Peter Lorentzen and Dr. Karen M. Park for helpful information on the case studies.

Conflict of Interest statement. None declared.

Funding

This work was supported by AIRC (IG-15208 to A.M.), MIUR (Progetto Bandiera Epigenomica—EPIGEN), Telethon (GGP12007 to A.M. and GGP14074 to E.B.) and the ONLUS Insieme per la Ricerca (PCDH19 to E.B.).

References

1. Rothbart, S.B. and Strahl, B.D. (2014) Interpreting the language of histone and DNA modifications. *Biochim. Biophys. Acta*, **1839**, 627–643.
2. Mosammaparast, N., Kim, H., Laurent, B., Zhao, Y., Lim, H.J., Majid, M.C., Dango, S., Luo, Y., Hempel, K., Sowa, M.E. *et al.* (2013) The histone demethylase LSD1/KDM1A promotes the DNA damage response. *J. Cell Biol.*, **203**, 457–470.
3. Laugesen, A. and Helin, K. (2014) Chromatin repressive complexes in stem cells, development, and cancer. *Cell Stem Cell*, **14**, 735–751.
4. Metzger, E., Wissmann, M., Yin, N., Muller, J.M., Schneider, R., Peters, A.H., Gunther, T., Buettner, R. and Schule, R. (2005) LSD1 demethylates repressive histone marks to promote androgen-receptor-dependent transcription. *Nature*, **437**, 436–439.
5. Herz, H.M., Morgan, M., Gao, X., Jackson, J., Rickels, R., Swanson, S.K., Florens, L., Washburn, M.P., Eissenberg, J.C. and Shilatifard, A. (2014) Histone H3 lysine-to-methionine mutants as a paradigm to study chromatin signaling. *Science*, **345**, 1065–1070.
6. Shen, E., Shulha, H., Weng, Z. and Akbarian, S. (2014) Regulation of histone H3K4 methylation in brain development and disease. *Philos. Trans. R. Soc. Lond. B Biol. Sci.*, **369**, 20130514.
7. Jensen, L.R., Amende, M., Gurok, U., Moser, B., Gimmel, V., Tzschach, A., Janecke, A.R., Tariverdian, G., Chelly, J., Fryns, J.P. *et al.* (2005) Mutations in the JARID1C gene, which is involved in transcriptional regulation and chromatin remodeling, cause X-linked mental retardation. *Am. J. Hum. Genet.*, **76**, 227–236.
8. Kleefstra, T., Brunner, H.G., Amiel, J., Oudakker, A.R., Nillesen, W.M., Magee, A., Genevieve, D., Cormier-Daire, V., van Esch, H., Fryns, J.P. *et al.* (2006) Loss-of-function mutations in euchromatin histone methyl transferase 1 (EHMT1) cause the 9q34 subtelomeric deletion syndrome. *Am. J. Hum. Genet.*, **79**, 370–377.
9. Rusconi, F., Paganini, L., Braida, D., Ponzoni, L., Toffolo, E., Maroli, A., Landsberger, N., Bedogni, F., Turco, E., Pattini, L. *et al.* (2015) LSD1 neurospecific alternative splicing controls neuronal excitability in mouse models of epilepsy. *Cereb Cortex*, **25**, 2729–2740.
10. Saleque, S., Kim, J., Rooke, H.M. and Orkin, S.H. (2007) Epigenetic regulation of hematopoietic differentiation by Gfi-1 and Gfi-1b is mediated by the cofactors CoREST and LSD1. *Mol. Cell*, **27**, 562–572.
11. Hojfeldt, J.W., Agger, K. and Helin, K. (2013) Histone lysine demethylases as targets for anticancer therapy. *Nat. Rev. Drug Discov.*, **12**, 917–930.
12. Chong, J.X., Yu, J.H., Lorentzen, P., Park, K.M., Jamal, S.M., Tabor, H.K., Rauch, A., Saenz, M.S., Boltshauser, E., Patterson, K.E. *et al.* (2015) Gene discovery for Mendelian conditions via social networking: de novo variants in KDM1A cause developmental delay and distinctive facial features. *Genet. Med.*, 10.1038/gim.2015.161.
13. Tunovic, S., Barkovich, J., Sherr, E.H. and Slavotinek, A.M. (2014) De novo ANKRD11 and KDM1A gene mutations in a male with features of KBG syndrome and Kabuki syndrome. *Am. J. Med. Genet. A*, **164**, 1744–1749.

14. Rauch, A., Wieczorek, D., Graf, E., Wieland, T., Endele, S., Schwarzmayr, T., Albrecht, B., Bartholdi, D., Beygo, J., Di Donato, N. *et al.* (2012) Range of genetic mutations associated with severe non-syndromic sporadic intellectual disability: an exome sequencing study. *Lancet*, **380**, 1674–1682.
15. Wang, J., Hevi, S., Kurash, J.K., Lei, H., Gay, F., Bajko, J., Su, H., Sun, W., Chang, H., Xu, G. *et al.* (2009) The lysine demethylase LSD1 (KDM1) is required for maintenance of global DNA methylation. *Nat. Genet.*, **41**, 125–129.
16. Wang, J., Scully, K., Zhu, X., Cai, L., Zhang, J., Prefontaine, G.G., Krones, A., Ohgi, K.A., Zhu, P., Garcia-Bassets, I. *et al.* (2007) Opposing LSD1 complexes function in developmental gene activation and repression programmes. *Nature*, **446**, 882–887.
17. Forneris, F., Binda, C., Vanoni, M.A., Mattevi, A. and Battaglioli, E. (2005) Histone demethylation catalysed by LSD1 is a flavin-dependent oxidative process. *FEBS Lett.*, **579**, 2203–2207.
18. Li, M., Binda, C., Mattevi, A. and Edmondson, D.E. (2006) Functional role of the "aromatic cage" in human monoamine oxidase B: structures and catalytic properties of Tyr435 mutant proteins. *Biochemistry*, **45**, 4775–4784.
19. Pilotto, S., Speranzini, V., Tortorici, M., Durand, D., Fish, A., Valente, S., Forneris, F., Mai, A., Sixma, T.K., Vachette, P. *et al.* (2015) Interplay among nucleosomal DNA, histone tails, and corepressor CoREST underlies LSD1-mediated H3 demethylation. *Proc. Natl. Acad. Sci. U. S. A.*, **112**, 2752–2757.
20. Shi, Y.J., Matson, C., Lan, F., Iwase, S., Baba, T. and Shi, Y. (2005) Regulation of LSD1 histone demethylase activity by its associated factors. *Mol. Cell*, **19**, 857–864.
21. Lee, M.G., Wynder, C., Bochar, D.A., Hakimi, M.A., Cooch, N. and Shiekhattar, R. (2006) Functional interplay between histone demethylase and deacetylase enzymes. *Mol. Cell. Biol.*, **26**, 6395–6402.
22. Zibetti, C., Adamo, A., Binda, C., Forneris, F., Toffolo, E., Verpelli, C., Ginelli, E., Mattevi, A., Sala, C. and Battaglioli, E. (2010) Alternative splicing of the histone demethylase LSD1/KDM1 contributes to the modulation of neurite morphogenesis in the mammalian nervous system. *J. Neurosci.*, **30**, 2521–2532.
23. Forneris, F., Binda, C., Vanoni, M.A., Battaglioli, E. and Mattevi, A. (2005) Human histone demethylase LSD1 reads the histone code. *J. Biol. Chem.*, **280**, 41360–41365.
24. Toffolo, E., Rusconi, F., Paganini, L., Tortorici, M., Pilotto, S., Heise, C., Verpelli, C., Tedeschi, G., Maffioli, E., Sala, C. *et al.* (2014) Phosphorylation of neuronal Lysine-Specific Demethylase 1LSD1/KDM1A impairs transcriptional repression by regulating interaction with CoREST and histone deacetylases HDAC1/2. *J. Neurochem.*, **128**, 603–616.
25. Lee, M.G., Wynder, C., Cooch, N. and Shiekhattar, R. (2005) An essential role for CoREST in nucleosomal histone 3 lysine 4 demethylation. *Nature*, **437**, 432–435.
26. Shen, C., Wang, D., Liu, X., Gu, B., Du, Y., Wei, F.Z., Cao, L.L., Song, B., Lu, X., Yang, Q. *et al.* (2015) SET7/9 regulates cancer cell proliferation by influencing beta-catenin stability. *FASEB J.*, **29**, 4313–4323.
27. Cano, A., Perez-Moreno, M.A., Rodrigo, I., Locascio, A., Blanco, M.J., del Barrio, M.G., Portillo, F. and Nieto, M.A. (2000) The transcription factor Snail controls epithelial-mesenchymal transitions by repressing E-cadherin expression. *Nat. Cell Biol.*, **2**, 76–83.
28. Baron, R., Binda, C., Tortorici, M., McCammon, J.A. and Mattevi, A. (2011) Molecular mimicry and ligand recognition in binding and catalysis by the histone demethylase LSD1-CoREST complex. *Structure*, **19**, 212–220.
29. Lin, Y., Wu, Y., Li, J., Dong, C., Ye, X., Chi, Y.I., Evers, B.M. and Zhou, B.P. (2010) The SNAG domain of Snail1 functions as a molecular hook for recruiting lysine-specific demethylase 1. *EMBO J.*, **29**, 1803–1816.
30. Barrallo-Gimeno, A. and Nieto, M.A. (2009) Evolutionary history of the snail/scratch superfamily. *Trends Genet.*, **25**, 248–252.
31. Whyte, W.A., Bilodeau, S., Orlando, D.A., Hoke, H.A., Frampton, G.M., Foster, C.T., Cowley, S.M. and Young, R.A. (2012) Enhancer decommissioning by LSD1 during embryonic stem cell differentiation. *Nature*, **482**, 221–225.
32. Foster, C.T., Dovey, O.M., Lezina, L., Luo, J.L., Gant, T.W., Barlev, N., Bradley, A. and Cowley, S.M. (2010) Lysine-specific demethylase 1 regulates the embryonic transcriptome and CoREST stability. *Mol. Cell. Biol.*, **30**, 4851–4863.
33. Nottke, A., Colaiacovo, M.P. and Shi, Y. (2009) Developmental roles of the histone lysine demethylases. *Development*, **136**, 879–889.
34. Thambyrajah, R., Mazan, M., Patel, R., Moignard, V., Stefanska, M., Marinopoulou, E., Li, Y., Lancrin, C., Clapes, T., Moroy, T. *et al.* (2016) GFI1 proteins orchestrate the emergence of haematopoietic stem cells through recruitment of LSD1. *Nat. Cell Biol.*, **18**, 21–32.
35. Huang, J., Sengupta, R., Espejo, A.B., Lee, M.G., Dorsey, J.A., Richter, M., Opravil, S., Shiekhattar, R., Bedford, M.T., Jenuwein, T. *et al.* (2007) p53 is regulated by the lysine demethylase LSD1. *Nature*, **449**, 105–108.
36. Laurent, B., Ruitu, L., Murn, J., Hempel, K., Ferrao, R., Xiang, Y., Liu, S., Garcia, B.A., Wu, H., Wu, F. *et al.* (2015) A specific LSD1/KDM1A isoform regulates neuronal differentiation through H3K9 demethylation. *Mol. Cell*, **57**, 957–970.
37. Wang, J., Telese, F., Tan, Y., Li, W., Jin, C., He, X., Basnet, H., Ma, Q., Merkurjev, D., Zhu, X. *et al.* (2015) LSD1n is an H4K20 demethylase regulating memory formation via transcriptional elongation control. *Nat. Neurosci.*, **18**, 1256–1264.
38. Wasson, J.A., Simon, A.K., Myrick, D.A., Wolf, G., Driscoll, S., Pfaff, S.L., Macfarlan, T.S. and Katz, D.J. (2016) Maternally provided LSD1/KDM1A enables the maternal-to-zygotic transition and prevents defects that manifest postnatally. *Elife*, **5**, 10.7554/eLife.08848.
39. Forneris, F., Binda, C., Adamo, A., Battaglioli, E. and Mattevi, A. (2007) Structural basis of LSD1-CoREST selectivity in histone H3 recognition. *J. Biol. Chem.*, **282**, 20070–20074.
40. Forneris, F., Orru, R., Bonivento, D., Chiarelli, L.R. and Mattevi, A. (2009) ThermoFAD, a Thermofluor-adapted flavin ad hoc detection system for protein folding and ligand binding. *FEBS J.*, **276**, 2833–2840.
41. Kabsch, W. (2010) Xds. *Acta Crystallogr. D Biol. Crystallogr.*, **66**, 125–132.
42. Winn, M.D., Ballard, C.C., Cowtan, K.D., Dodson, E.J., Emsley, P., Evans, P.R., Keegan, R.M., Krissinel, E.B., Leslie, A.G., McCoy, A. *et al.* (2011) Overview of the CCP4 suite and current developments. *Acta Crystallogr. D Struct. Biol.*, **67**, 235–242.
43. Rusconi, F., Mancinelli, E., Colombo, G., Cardani, R., Da Riva, L., Bongarzone, I., Meola, G. and Zippel, R. (2010) Proteome profile in myotonic dystrophy type 2 myotubes reveals dysfunction in protein processing and mitochondrial pathways. *Neurobiol. Dis.*, **38**, 273–280.
44. Karplus, P.A. and Diederichs, K. (2012) Linking crystallographic model and data quality. *Science*, **336**, 1030–1033.